Rapid Communications

Polar flock in the presence of random quenched rotators

Rakesh Das,[1,*] Manoranjan Kumar,[1,†] and Shradha Mishra[2,‡]
[1]*S. N. Bose National Centre for Basic Sciences, Block JD, Sector III, Salt Lake, Kolkata 700106, India*
[2]*Department of Physics, Indian Institute of Technology (BHU), Varanasi 221005, India*

(Received 20 March 2018; revised manuscript received 5 June 2018; published 14 December 2018)

We study a collection of polar self-propelled particles (SPPs) on a two-dimensional substrate in the presence of random quenched rotators. These rotators act like obstacles which rotate the orientation of the SPPs by an angle determined by their intrinsic orientations. In the zero self-propulsion limit, our model reduces to the equilibrium XY model with quenched disorder, while for the clean system, it is similar to the Vicsek model for polar flock. We note that a small amount of the quenched rotators destroys the long-range order usually noted in the clean SPPs. The system shows a quasi-long range order state upto some moderate density of the rotators. On further increment in the density of rotators, the system shows a continuous transition from the quasi-long-range order to disorder state at some critical density of rotators. Our linearized hydrodynamic calculation predicts anisotropic higher order fluctuation in two-point structure factors for density and velocity fields of the SPPs. We argue that nonlinear terms probably suppress this fluctuation such that no long-range order but only a quasi-long-range order prevails in the system.

DOI: 10.1103/PhysRevE.98.060602

Flocking of self-propelled particles (SPPs) is an ubiquitous phenomenon in nature. The size of these flocks ranges from a few microns to the order of a few kilometers, e.g., bacterial colony, cytoskeleton, shoal of fishes, animal herds, where the individual constituent shows systematic movement at the cost of its free energy. Since the seminal work by Vicsek *et al.* [1], numerous works are done to understand the flocking phenomena of SPPs [2–6]. One of the interesting features of these kinds of out-of-equilibrium systems is the realization of true long-range order (LRO) even in two dimensions (2D) [7,8]. Most of the previous analytical and numerical studies of SPPs were restricted to homogeneous or clean systems [1,7–10]. However, natural systems in general have some kind of inhomogeneity. Therefore, some of the recent studies focus on the effects of different kinds of inhomogeneities present in the systems [11–15]. The study in Ref. [11] shows the breakdown of the flocking state of artificially designed SPPs in the presence of randomly placed circular obstacles. In Ref. [12], Chepizhko *et al.* model obstacles such that the SPPs avoid those obstacles. They note a surprising nonmonotonicity in the isotropic to flocking state transition of the SPPs in the presence of the obstacles. They also report a transition from LRO to quasi-long-range order (QLRO) state at some nonzero but finite density of obstacles. While commenting about these studies, the authors of Ref. [16] stress upon the understanding of the flocking phenomena in the presence of different kinds of inhomogeneities. In the same spirit, we study the effect of rotator type obstacles on the nature of ordering in polar SPPs. Moreover, we propose a minimal model for SPPs in inhomogeneous medium, the results for which could easily be compared with its well-studied equilibrium counterpart [17,18].

In this Rapid Communication, we consider a Vicsek-like model [1] of polar SPPs in the presence of obstacles in the medium. The obstacles are modeled as random quenched rotators which rotate the orientation of neighboring SPPs by an angle determined by the intrinsic orientations of the rotators. The model can be visualized as a large moving crowd, amid which some random "road signs" have been placed. Individual road sign dictates the neighboring people to take a roundabout by a certain angle from their direction of motion. The specific issue we address here is the correlation of this collective motion in the presence of these random road signs.

In the limit of zero self-propulsion speed, our model reduces to the XY model [19] with random quenched obstacles. In the XY model, any finite amount of quenched randomness is enough to destroy the orientationally ordered state in dimension $d \leqslant 4$ [17,18]. Therefore in 2D, an equilibrium system with quenched obstacles does not have any ordered state. Analogous to this, we show that in a two-dimensional self-propelled system, quenched rotators destroy the LRO, usually found in the clean polar SPPs.

In our numerical study, we note that small density of quenched rotators leads the system to a QLRO state. In this state, the absolute value of average normalized velocity V decreases algebraically with the system size. Also, fluctuation in the orientations of the SPPs increases logarithmically with system size. Moreover, below a critical density of rotators c_{rc}, both V and fluctuation in orientations of SPPs show nice scaling collapse with scaled system size. However, with further increase in density of rotators c_r, the system shows a continuous QLRO to disorder (QLRO-disorder) state transition. We also write hydrodynamic equations of motion for density and velocity fields of the SPPs in the presence of quenched inhomogeneities. A linearized study of these equations predicts an

*rakesh.das@bose.res.in
†manoranjan.kumar@bose.res.in
‡smishra.phy@itbhu.ac.in

anisotropic divergence of $\mathcal{O}(1/q^4)$ in the equal-time spatially Fourier transformed correlations for the hydrodynamic fields for small q. However, neglected nonlinear terms probably suppress these fluctuations to make the QLRO possible in the system.

We consider a collection of N_s polar SPPs distributed over a 2D square substrate. Each particle moves with a fixed speed v_s along its orientation ϕ. An individual SPP tries to reorient itself along the mean orientation of all the neighboring SPPs (including itself) within an interaction radius R_s. However, ambience noise leads to orientational perturbation. Moreover, there are N_r immobile rotators randomly distributed on the substrate. Each rotator possesses an intrinsic orientation φ, which can take any random value in the range $[-\pi, \pi]$ and remains fixed. Therefore, the rotators are quenched in time, and we call these random quenched rotators (RQRs). Each RQR rotates the orientations of the SPPs within an interaction radius R_r by an angle determined by φ and SPP-RQR interaction strength μ. The update rules governing position $\boldsymbol{r}_i$ and orientation ϕ_i of the ith SPP are as follows:

$$\boldsymbol{r}_i(t+1) = \boldsymbol{r}_i(t) + \boldsymbol{v}_i(t), \tag{1}$$

$$\phi_i(t+1) = \langle \phi_j(t) \rangle_{j \in R_s} + \mu \langle \varphi_j \rangle_{j \in R_r} + \Delta\psi, \tag{2}$$

where $\boldsymbol{v}_i(t) = v_s(\cos\phi_i(t), \sin\phi_i(t))$ is the velocity of the particle i at time t, and $\langle\phi\rangle_{R_s}$ and $\langle\varphi\rangle_{R_r}$ represent the mean orientation of all the SPPs and the RQRs, respectively, within the interaction radii. Fluctuation in orientation of SPPs because of ambience noise is represented by an additive noise term $\Delta\psi$ distributed within $\eta[-\pi, \pi]$, where noise strength $\eta \in [0, 1]$. We call this model "active model with quenched rotators (AMQR)," which reduces to the celebrated Vicsek model [1] for $\mu = 0$ or in the clean system, i.e., $N_r = 0$.

We numerically simulate the collection of N_s SPPs spread over the $L \times L$ ($L \in [50, 300]$) 2D substrate with periodic boundary condition. Initially the particles are chosen to have random velocity, but with constant speed v_s. The density of the SPPs and the RQRs are defined as $c_s = N_s/L^2$ and $c_r = N_r/L^2$, respectively. We distribute these rotators uniformly on the substrate, and randomly assign intrinsic orientation $\varphi \in [-\pi, \pi]$. In this system, the position and the velocity of all the SPPs are updated simultaneously following Eqs. (1) and (2). At every time step, we use OpenMP Application Program Interface for a parallel updating procedure of all the SPPs.

In this Rapid Communication, we consider $c_s = 1.0$, $v_s = 1.0$, and $\mu = 1.0$. Moreover, we take $R_s = R_r = 1$ for simplicity. In the absence of the rotators [1], the system shows disorder to order transition with decreasing noise strength η. The ordering in the system is measured in terms of the conventional absolute value of the average normalized velocity

$$V = \left\langle \frac{1}{N_s v_s} \left| \sum_{i=1}^{N_s} \boldsymbol{v}_i \right| \right\rangle \tag{3}$$

of the entire system [1]. Here $\langle\cdot\rangle$ indicates an average over many realizations and time in the steady state. V varies from zero to unity for disorder to order state transition. For the reported data, we start the averaging of observables after 3×10^5 updates to assure reaching the steady state, and averaging is done for the next 5×10^5 updates. Up to 30 realizations are used for better averaging.

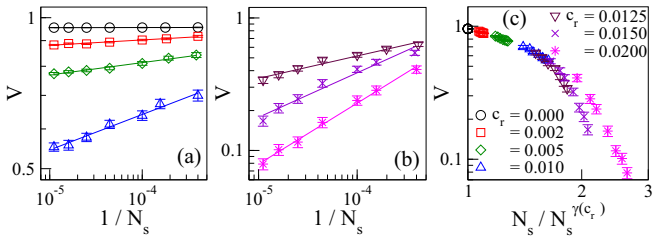

FIG. 1. V versus $1/N_s$ plots in the (a) ordered and (b) disordered state for $\eta = 0.10$. The error bars indicate standard error in mean. The solid lines show the respective algebraic fits. (c) Plot of V versus scaled system size N_s/N_s^{γ} on log-log scale, where γ is a function of c_r. The data shows good scaling for $0 < c_r \leqslant 0.0125$, but deviates for $c_r \geqslant 0.0125$.

For a fixed η, we calculate V for different c_r, and study its variation with system size. As shown for $\eta = 0.1$ in Fig. 1(a), in the clean system, V does not change with system size; consequently, the system possesses a nonzero V in the thermodynamic limit. Therefore, the clean system remains in the LRO state, which is a well-known phenomenon [8]. However, in the presence of the RQRs, V decreases algebraically with N_s following the relation

$$V = \mathcal{A}(c_r) N_s^{-\nu(c_r)}, \tag{4}$$

as shown in Figs. 1(a) and 1(b). Here both $\mathcal{A}$ and ν are functions of c_r for a fixed η. Therefore, in the thermodynamic limit, V of the system with RQRs reduces to zero. We stress that for small c_r the system remains in a QLRO state, beyond which the AMQR shows a continuous QLRO-disorder state transition, as we will see shortly. In Fig. 2, we show snapshots of the orientation and the local density of the SPPs for $\eta = 0.1$ and different c_r. For $c_r = 0$, all the particles are in highly ordered state. RQRs perturb the LRO flocking as shown for $c_r = 0.005, 0.01$. For high density $c_r = 0.02$, the SPPs remain highly disordered.

We further study the fluctuation in the orientation of the SPPs. The width of a normalized distribution $P(\phi)$ of orientation of the SPPs provides a measure of this fluctuation. It is calculated by averaging over the distributions at every time step in the steady state, and also over many realizations. While averaging, we set the mean orientation of all the distributions at $\phi = 0$.

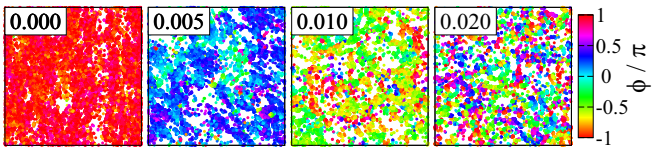

FIG. 2. Steady-state snapshots are shown for $\eta = 0.10$, $L = 150$ and different c_r as indicated on the respective panels. The color bar indicates orientation of the SPPs. The rotators with random intrinsic orientation are not shown for the clarity of the figure.

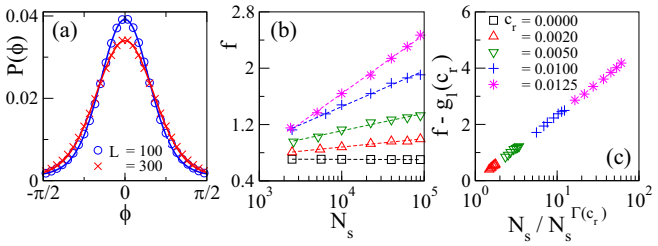

FIG. 3. (a) Distribution $P(\phi)$ of the orientation of the SPPs is shown for $\eta = 0.10$ and $c_r = 0.005$. The curves are zoomed into the range $\phi \in [-\pi/2, \pi/2]$ for better visibility. The solid lines show the respective fits with Voigt profile. (b) Plot of the FWHM f of $P(\phi)$ versus N_s. In the presence of quenched rotators, f increases logarithmically with N_s. The dashed lines show respective fits. (c) Plot of shifted FWHM $f - g_1(c_r)$ with scaled system size N_s/N_s^{Γ}, where both g_1 and Γ are functions of c_r. The scaling holds good for $c_r \leqslant 0.0125$.

We note that $P(\phi)$ widens with the increasing density of RQRs. This is quite intuitive since the degree of disorder increases with c_r. We fit these distributions with a Voigt profile, which is defined as the convolution of the Gaussian and the Lorentzian functions [20]. A brief discussion of the Voigt profile and the procedure used to fit $P(\phi)$ with it are provided in the Supplemental Material [21]. From the respective fits, we calculate the full width at half maximum (FWHM) f of the distributions.

We note that, in the clean system, $P(\phi)$ does not change with system size. However, for any fixed $c_r > 0$, $P(\phi)$ widens with increasing system size, as shown in Fig. 3(a) for $(\eta, c_r) = (0.10, 0.005)$ (also see the Supplemental Material [21]). In Fig. 3(b), we show the variation of f with system size for different c_r. For $c_r = 0$, f does not change with N_s. Therefore, in the clean system, the fluctuation in the orientation of the SPPs does not depend on the system size, and the system is in the LRO state. However, for $c_r > 0$, FWHM of $P(\phi)$ follows the relation $f = g_1(c_r) + g_2(c_r)\ln(N_s)$, where both g_1 and g_2 are functions of c_r. Since $g_2 \geqslant 0$, f increases logarithmically with N_s, which further confirms the QLRO in the AMQR.

In Fig. 1(c), we plot V versus scaled system size $N_s/N_s^{\gamma(c_r)}$ for $\eta = 0.1$ and different c_r. Here $\gamma(c_r) \simeq 1 - kc_r$, where k is a positive constant. Moreover, $\nu = z(1-\gamma)$, where z is a nonmonotonic function of η. We note nice scaling collapse for $c_r \leqslant 0.0125$. This predicts that, for $c_r \leqslant 0.0125$, the system can be divided into subsystems of size $N_s^{\gamma(c_r)}$ within which the SPPs remain ordered. Since $\gamma = 1$ for $c_r = 0$, V does not depend on system size, and therefore the clean system remains in the LRO state. However, in the presence of RQRs, the system remains in the QLRO state. Moreover, the scaling predicts self-similarity of the system for different $c_r \leqslant 0.0125$. As shown in Fig. 3(c), we also find nice scaling collapse of $f - g_1(c_r)$ with scaled system size $N_s/N_s^{\Gamma(c_r)}$ for different $c_r \leqslant 0.0125$, where $\Gamma = 1 - g_2$ that varies linearly with c_r, for small c_r. Similar scaling holds for other η values in the QLRO state.

In Fig. 4(a), we show the variation of V with c_r for $\eta = 0.1$ and different system sizes. Starting from the value of V close to 1 for small c_r, V shows a transition to smaller values with

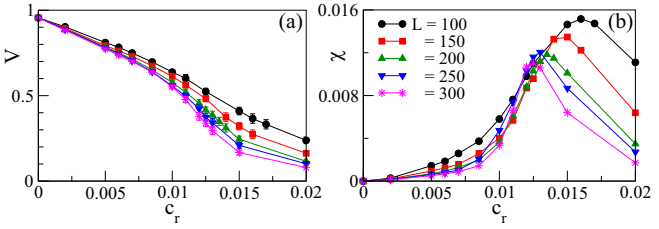

FIG. 4. (a) Variation of V with c_r shown for different system sizes and $\eta = 0.10$. (b) Variance χ of V plotted with c_r. The peaks in the curves indicate the critical density of the rotators $c_{rc}(L)$ for the QLRO-disorder transition for the respective system sizes.

increasing c_r. Therefore, with increasing c_r, QLRO-disorder transition occurs in the system. We further calculate the variance χ of V for different system sizes, and plot these as a function of c_r in Fig. 4(b). Data shows systematic variation in χ as a function of c_r, and a peak appears at $c_r = c_{rc}(L)$ where the fluctuation in V is large. This suggests a continuous QLRO-disorder state transition in the AMQR. We consider $c_{rc}(L)$ as the critical density for the QLRO-disorder state transition for system size L. The position of the peak shifts from $c_r = 0.016$ to 0.0125 as L is increased from 100 to 300. However, we note that $c_{rc}(L)$ flattens on increasing L for all η values. Using the extrapolated values $c_{rc}(L \to \infty)$, we construct a phase diagram in the η–c_r plane. We stress that in the presence of RQRs, the system remains in the QLRO below the phase boundary shown in Fig. 5.

Long-distance and long-time properties of the SPPs with quenched obstacles can also be characterized using a hydrodynamic description of the model. The relevant hydrodynamic variables for this model are (i) SPP density $\rho(\boldsymbol{r}, t)$ which is a globally conserved quantity and (ii) velocity $\boldsymbol{v}(\boldsymbol{r}, t)$ which is a broken-symmetry parameter in the ordered state. These variables can be obtained by suitable coarsening of corresponding discrete variables in the microscopic model [7,8,22–25]. Following the phenomenology of the system, we write the hydrodynamic equations of motion for the density and the velocity fields as

$$\partial_t \rho + \nabla \cdot (\boldsymbol{v}\rho) = D_\rho \nabla^2 \rho, \tag{5}$$

$$\begin{aligned} \partial_t \boldsymbol{v} + \lambda_1(\boldsymbol{v}\cdot\nabla)\boldsymbol{v} + \lambda_2(\nabla\cdot\boldsymbol{v})\boldsymbol{v} + \lambda_3\nabla(v^2) \\ = (\alpha_1 - \alpha_2 v^2)\boldsymbol{v} - \nabla P + D_B\nabla(\nabla\cdot\boldsymbol{v}) \\ + D_T\nabla^2\boldsymbol{v} + D_2(\boldsymbol{v}\cdot\nabla)^2\boldsymbol{v} + \frac{\rho_o}{\rho}\boldsymbol{\zeta} + \boldsymbol{f}. \end{aligned} \tag{6}$$

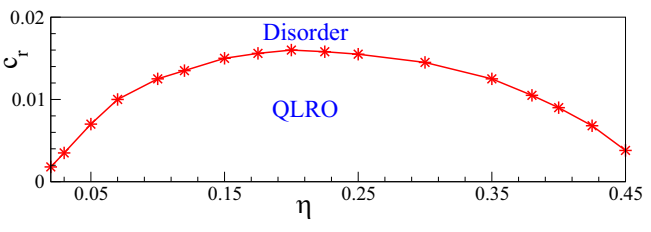

FIG. 5. Phase diagram in noise strength versus density of rotator plane. For small c_r, the QLRO state prevails, beyond which the system continuously goes to the disorder state.

$\boldsymbol{f}$ represents the annealed noise term that provides a random driving force. We assume this to be a white Gaussian noise with the correlation

$$\langle f_i(\boldsymbol{r},t)f_j(\boldsymbol{r}',t')\rangle = \Delta\delta_{ij}\delta(\boldsymbol{r}-\boldsymbol{r}')\delta(t-t'), \tag{7}$$

where Δ is a constant, and dummy indices i, j denote Cartesian components. The effect of obstacles is contained in the term $\frac{\rho_o}{\rho}\boldsymbol{\zeta}$ in Eq. (6), where ρ_o represents obstacle density, and $\boldsymbol{\zeta}(\boldsymbol{r},t)$ signifies the obstacle field. We assume the correlation

$$\langle \zeta_i(\boldsymbol{r},t)\zeta_j(\boldsymbol{r}',t')\rangle = \zeta^2\delta_{ij}\delta(\boldsymbol{r}-\boldsymbol{r}'), \tag{8}$$

which contains no time dependence, and therefore represents a quenched noise. Equations (5)–(8) represent the Toner-Tu [8] model for $\zeta = 0$.

We check whether a broken-symmetry state of the SPPs in the presence of the obstacle field survives to small fluctuation in the hydrodynamic fields. In the hydrodynamic limit, a linearized study of Eqs. (5) and (6) gives spatially Fourier transformed equal-time correlation functions for the density

$$C_{\rho\rho}(\boldsymbol{q},t) = \frac{1}{q^2}\left\{\frac{\zeta^2\rho_o^2 a_\rho(\theta)}{b(\theta)q^2+d(\theta)} + \Delta A_\rho(\theta)\right\} \tag{9}$$

and the velocity

$$C_{vv}(\boldsymbol{q},t) = \frac{1}{q^2}\left\{\frac{\zeta^2\rho_o^2 a_v(\theta)}{b(\theta)q^2+d(\theta)} + \Delta A_v(\theta)\right\}. \tag{10}$$

The parameters $a_{\rho,v}$, $A_{\rho,v}$, b, and d depend on the specific microscopic model and the angle θ between the wave number $\boldsymbol{q}$ and the flocking direction. A detailed calculation for Eqs. (9) and (10) is given in the Supplemental Material [21]. Our result matches with the earlier prediction by Toner and Tu [8] for $\zeta = 0$, where the two structure factors diverge as $1/q^2$ for small q. However, the linearized theory suggests $C_{\rho\rho,vv} \sim 1/q^4$ for $\zeta \neq 0$, provided $d(\theta) = 0$. In general for a Vicsek-like model as our AMQR, $d(\theta)$ vanishes for certain directions $\theta = \theta_c$ or $\pi - \theta_c$, where θ_c depends on the model parameters. We stress that although the quenched inhomogeneities increase fluctuation in the system as compared to the clean case, the neglected nonlinearities suppress these higher order fluctuations so that a QLRO state can prevail. Although an exact nonlinear calculation is *not practically feasible* for the 2D polar flock [26], presumption of convective nonlinearities as relevant terms offers a way out [3,8]. A nonlinear calculation [26] following this presumption renormalizes diffusivities as $1/q$ so that the term $b(\theta)q^2$ in Eqs. (9) and (10) approaches a finite value, and therefore, a QLRO state exists in the system. This explanation is consistent with the giant number fluctuation [4] in the AMQR. We have checked that inclusion of the RQRs increases the fluctuation in the system as compared to the clean case. This enhanced fluctuation destroys the usual LRO of the clean system. However, we note that the fluctuation decreases with further increase in c_r which disagrees with Eq. (9), as the linearized hydrodynamics prescribes an increase in the effect of quenched inhomogeneity with ρ_o. Therefore, the neglected nonlinearity indeed plays a pivotal role in stabilizing the QLRO state in the system. A detailed discussion of these phenomenologies is given in the Supplemental Material [21].

In summary, we have studied the effect of random quenched rotators on the flocking state of polar SPPs. These rotators are one kind of obstacle that rotate the orientation of the SPPs. We find that, for small density of the rotators, the usual LRO of the clean polar SPPs is destroyed, and a QLRO state prevails. With further increase in density of the rotators, a continuous QLRO to disorder state transition takes place in the system. Our linearized hydrodynamic analysis predicts an anisotropic higher order fluctuation which destroys the usual LRO of the clean SPPs. However, the neglected nonlinearities suppress these fluctuations yielding a QLRO in the system. In equilibrium systems with random quenched obstacles, an ordered state does not exist below four dimensions [17,18]. However, as compared to the equilibrium systems, in our model for polar SPPs with quenched rotators, we find QLRO in two dimensions. Our prediction of the QLRO in the polar SPPs in the presence of quenched obstacles agrees with recent observations [12,26].

In contrast to the LRO and the QLRO reported in Ref. [12], we note QLRO only, because of the basic difference in the nature of obstacles. The SPP-obstacle interaction in Ref. [12] depends on the angle between their relative position vector and the orientation of the SPP. Therefore, this force is a continuous function of the orientation distribution of the SPPs. On the contrary, the quenched force offered by the obstacles in our model is random and discrete. However, similar to their results, we note the existence of an optimal noise for which the system attains the maximum ordering in the presence of quenched rotators (see the Supplemental Material [21]). Our model can be applied in natural systems like a shoal of fishes moving in the sea in the presence of vortices. An experiment on a collection of fishes living in a shallow water pool [27–30], in the presence of uncorrelated artificial vortices, may verify our predictions.

S.M. acknowledges Sriram Ramaswamy for pointing out an important correction in the hydrodynamic calculation and Sanjay Puri for useful discussions. The authors thank John Toner for his useful comments and suggestions. S.M. also thanks S. N. Bose National Centre for Basic Sciences, Kolkata for providing kind hospitality, and the Department of Science and Technology, India for financial support. M.K. acknowledges financial support from the Department of Science and Technology, India under the Ramanujan Fellowship.

[1] T. Vicsek, A. Czirók, E. Ben-Jacob, I. Cohen, and O. Shochet, Phys. Rev. Lett. **75**, 1226 (1995).

[2] M. C. Marchetti, J. F. Joanny, S. Ramaswamy, T. B. Liverpool, J. Prost, M. Rao, and R. A. Simha, Rev. Mod. Phys. **85**, 1143 (2013).

[3] J. Toner, Y. Tu, and S. Ramaswamy, Ann. Phys. (NY) **318**, 170 (2005).

[4] S. Ramaswamy, Annu. Rev. Condens. Matter Phys. **1**, 323 (2010).

[5] T. Vicsek and A. Zafeiris, Phys. Rep. **517**, 71 (2012).

[6] M. E. Cates, Rep. Prog. Phys. **75**, 042601 (2012).
[7] J. Toner and Y. Tu, Phys. Rev. Lett. **75**, 4326 (1995).
[8] J. Toner and Y. Tu, Phys. Rev. E **58**, 4828 (1998).
[9] S. Mishra, A. Baskaran, and M. C. Marchetti, Phys. Rev. E **81**, 061916 (2010).
[10] H. Chaté, F. Ginelli, G. Grégoire, and F. Raynaud, Phys. Rev. E **77**, 046113 (2008).
[11] A. Morin, N. Desreumaux, J. B. Caussin, and D. Bartolo, Nat. Phys. **13**, 63 (2017).
[12] O. Chepizhko, E. G. Altmann, and F. Peruani, Phys. Rev. Lett. **110**, 238101 (2013).
[13] D. Yllanes, M. Leoni, and M. C. Marchetti, New J. Phys. **19**, 103026 (2017).
[14] D. A. Quint and A. Gopinathan, Phys. Biol. **12**, 046008 (2015).
[15] C. Sándor, A. Libál, C. Reichhardt, and C. J. Olson Reichhardt, Phys. Rev. E **95**, 032606 (2017).
[16] C. J. O. Reichhardt and C. Reichhardt, Nat. Phys. **13**, 10 (2017).
[17] Y. Imry and S. K. Ma, Phys. Rev. Lett. **35**, 1399 (1975).
[18] G. Grinstein and A. Luther, Phys. Rev. B **13**, 1329 (1976).
[19] P. M. Chaikin and T. C. Lubensky, *Principles of Condensed Matter Physics* (Cambridge University Press, Cambridge, 1998).
[20] J. J. Olivero and R. L. Longbothum, J. Quant. Spectrosc. Radiat. Transfer **17**, 233 (1977).
[21] See Supplemental Material at http://link.aps.org/supplemental/10.1103/PhysRevE.98.060602 for (i) Voigt profile and orientation fluctuation of SPPs, (ii) linearized hydrodynamics, (iii) effect of nonlinear terms, and (iv) optimal noise.
[22] A. Baskaran, J. W. Dufty, and J. J. Brey, Phys. Rev. E **77**, 031311 (2008).
[23] E. Bertin, M. Droz, and G. Grégoire, Phys. Rev. E **74**, 022101 (2006).
[24] E. Bertin, M. Droz, and G. Grégoire, J. Phys. A: Math. Theor. **42**, 445001 (2009).
[25] T. Ihle, Phys. Rev. E **83**, 030901(R) (2011).
[26] J. Toner, N. Guttenberg, and Y. Tu, arXiv:1805.10324v1; Phys. Rev. E **98**, 062604 (2018).
[27] D. J. T. Sumpter, J. Krause, R. James, I. D. Couzin, and A. J. W. Ward, Curr. Biol. **18**, 1773 (2008).
[28] J. W. Jolles, N. J. Boogert, V. H. Sridhar, I. D. Couzin, and A. Manica, Curr. Biol. **27**, 2862 (2017).
[29] L. Snijders, R. H. J. M. Kurvers, S. Krause, I. W. Ramnarine, and J. Krause, Nat. Ecol. Evol. **2**, 1610 (2018).
[30] J. G. Puckett, A. R. Pokhrel, and J. A. Giannini, Sci. Rep. **27**, 7587 (2018).